Journal of Materials Chemistry

Cite this: *J. Mater. Chem.*, 2012, **22**, 11503

www.rsc.org/materials

PAPER

Zippered release from polymer-gated carbon nanotubes†

Afnan Mashat,‡[a] Lin Deng,‡[a] Azza Altawashi,[b] Rachid Sougrat,[c] Guangchao Wang[c] and Niveen M. Khashab*[a]

Received 23rd January 2012, Accepted 22nd February 2012
DOI: 10.1039/c2jm30454f

A thermosensitive drug delivery system based on polymer-gated carbon nanotubes (CNTs) that are loaded with the anticancer drug doxorubicin (DOX) is herein reported. The development of carbon nanotubes for various biomedical applications is the research focus of many research groups and holds great promise. The major drawback of these materials is the toxicity that is associated with conjugated carbon systems. Functionalization of CNTs with polymers has proved very successful in lowering the toxicity and improving the pharmacokinetic profile. In this work, CNTs are coated with polyethylenimine (PEI) and polyvinyl alcohol (PVA) *via* the "zipper effect" that provides both support and control over drug release. PEI/PVA provides excellent support to increase DOX loading on the nanocarrier. The system is controlled by changes in temperature due to the complexation (low temperature) and decomplexation (high temperature) of PEI and PVA *via* hydrogen bonding. The release of DOX was tested in three cell lines (Lung fibroblast (LF), Breast Adenocarcinoma (BA), and HeLa). It was further tested in primary cell lines (Human Dermal Fibroblast adult (HDFa) and Human Dermal Fibroblast neonatal (HDFn)). When the bonds between PEI and PVA are decomplexed at high temperature (≥40 °C), drug release was observed as verified by fluorescence microscopy. There was no drug release at room temperature (25 °C) and a slow release at normal body temperature (37 °C). This system represents a promising method for incorporating stimuli triggered polymer-gated CNTs in future controlled release applications.

Introduction

Carbon nanotubes (CNTs) have special mechanical, electrical, thermal, physical and chemical properties that generated huge activities in many areas of science and engineering.[1–13] CNTs also exhibit several remarkable characteristics that make them ideal for biomedical applications such as drug and gene delivery and biosensors.[11,14–25] CNTs can penetrate the cell membranes[14,26] and their nano size makes them travel easily inside the body.[27] Moreover, it has been shown that the hollow tube structure of CNTs enhances the loading quantity, which possibly will increase the circulation time and consequently increase the bioavailability of the delivered drugs.[28–31] Recently, the inner and outer surfaces of CNTs were used for drug delivery by using covalent,[32] non-covalent[33] or electrostatic interactions.[34] Functionalization of CNTs is crucial to lower the toxicity and increase the biological accessibility associated with this material.[19] Coating with biocompatible polymers is one of the most important methods for functionalization or modification of CNTs.[35–38]

The "zipper effect" is a term used to describe the interaction between two polymers through hydrogen bonding.[39] Based on alternate deposition of polymers, one with a hydrogen bond acceptor and the other with a hydrogen bond donor, multilayer films can be formed.[40] The thickness and the morphology of the multilayer films can be changed depending on the interaction between the hydrogen bonds. This type of interaction is sensitive to temperature and thus increasing the temperature can lead to dissociation of hydrogen bonds.[39,41]

Controlling the release of cargo from a delivery vehicle is an important factor in the system's design as it greatly limits the side effects of excess release.[42] Several controlled release systems have been developed in the last few years. For instance, a photosensitive system was used to control the release of different molecules from coumarin-modified mesoporous materials.[43,44] A dual anion and pH controlled gate like system has been reported by using linear polyamines anchored on the outer surface of

[a]*Controlled Release and Delivery Lab (CRD), Advanced Membranes and Porous Materials Center, King Abdullah University of Science and Technology (KAUST), Thuwal, 23955-6900, Kingdom of Saudi Arabia. E-mail: niveen.khashab@kaust.edu.sa; Fax: +966-2-802-1172; Tel: +966-2-808-2410*

[b]*Chemical and Life Sciences and Engineering Division, King Abdullah University of Science and Technology (KAUST), Thuwal, 23955-6900, Kingdom of Saudi Arabia.*

[c]*Advanced Nanofabrication, Imaging and Characterization Core Facilities, King Abdullah University of Science and Technology (KAUST), Thuwal, 23955-6900, Kingdom of Saudi Arabia.*

† Electronic supplementary information (ESI) available: Calculation of DOX loading, thermogravimetric analysis, electron energy loss spectroscopy, Rhodamine B (RhB) release, cell viabilities of primary cells, TEM images of BA cells treated by DOX loaded CNTs–PEI/PVA. See DOI: 10.1039/c2jm30454f

‡ Both authors contributed equally to this work.

mesoporous materials.[45] A magnetic field based on nanocomposite membranes was also used to control the release of a drug by providing a reversible on-off system.[46] Other controlled release systems were triggered by pH,[47–50] enzymes,[51–53] light[54–57] and redox.[54,58]

Herein, a CNT-based temperature sensitive system is reported for controlled release applications. Polyethylenimine (PEI) and polyvinyl alcohol (PVA) were used to coat CNTs *via* the zipper effect. CNTs–PEI/PVA were successfully loaded with doxorubicin (DOX) and the release curves were tested at 25, 37, 40 and 70 °C. The designed system is thermosensitive, as it opens at 40 °C and closes (no release) at 25 °C while minor release is observed at 37 °C. *In vitro* testing was carried out to verify that the system is safe and suitable for drug delivery. The release profile proves that CNTs–PEI/PVA can successfully store DOX and release on demand by increasing the temperature to 40 °C. Increasing the temperature to 70 °C was only done to further verify the system experimental dependence on increasing temperature.

Experimental section

Synthesis of CNTs–PEI and CNTs–PEI/PVA

The functionalization of CNTs was accomplished as follows:[59,60] Carboxylic acid functionalized CNTs (CNTs–COOH) were added to oxalyl chloride and refluxed at 60 °C for 24 h to convert the carboxylic acids to acyl chlorides. The excess oxalyl chloride and other acidic products were removed under vacuum, and then PEI in anhydrous DMF was added and reacted at 40 °C for 24 h. CNTs–PEI were obtained after drying under vacuum overnight. PVA aqueous solution (2%) was added to the pre-dispersed CNTs–PEI aqueous solution. After stirring for 24 h, CNTs–PEI/PVA were formed *via* hydrogen bonding complexation between PVA and PEI (Fig. 1). The surface modification of each step was tested by thermogravimetric analysis (TGA) using a TG 209 F1 Iris (Netzsch Company) with a heating rate of 10 °C min^{-1} in nitrogen. Also, Raman spectra were recorded using a confocal micro-Raman spectrometer (Horiba Jobin Yvon/Labram Aramis) with an excitation wavelength of 473 nm.

DOX loading

CNTs–PEI/PVA (200 mg) were dispersed in 10 mL of water. Then, an aqueous solution of DOX was added and stirred at 40 °C for ~24 h. The sample was then cooled down in an ice bath for 2 h, washed by water (5 times), isolated by centrifugation, and finally the release was tested by fluorescence spectrophotometer. DOX loading efficiency was estimated by measuring the absorbance of unloaded DOX at 485 nm relative to the predefined calibration curve (ESI, Fig. S1†).

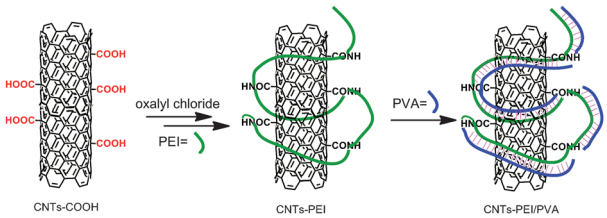

Fig. 1 Synthesis of polymer-gated CNTs.

DOX release from CNTs–PEI/PVA

DOX-loaded CNTs–PEI/PVA were tested at 25 °C, 37 °C, 40 °C and 70 °C in water. The fluorescence intensity of released DOX was determined by fluorescence spectrophotometer (Cary Eclipse) in the range of 520–650 nm when the excitation wavelength was set at 485 nm and continuous "on-off" (40 °C–25 °C) intensities are also recorded.

Cytotoxicity assay

The cytotoxicity was measured by the Alamar Blue reduction assay (Sigma) using human Lung fibroblast (LF), Breast Adenocarcinoma (BA) and HeLa lines (ATTC). Only living cells are able to manage the reduction of Alamar blue. Cells were cultivated in a 96 well microtiter plate 2×10^4 cell/well in Eagle's minimal essential medium (EMEM) + 10% Fetal Bovine Serum (FBS), 200 μL/well) at 37 °C in a humidified 5% carbon dioxide atmosphere. The cytotoxicity was also measured by LDH assay (Sigma) using LF, BA and HeLa cell lines and Human Dermal Fibroblast adult and neonatal (ATTC) (ESI†). The release of LDH is an indication of cell death. Cells were cultivated in a 96 well microtiter plate 2×10^4 cell/well in EMEM + 10% FBS, 200 μL/well) at 37 °C in a humidified 5% carbon dioxide atmosphere. The optical density was measured at 492 nm with a microplate reader. The mean of four measurements for each cell line was determined ($n = 4$).

In vitro drug uptake

Breast Adenocarcinoma (BA) cultured on poly-D-lysine-coated coverslips were treated with CNTs–PEI/PVA (50 μg mL^{-1}), fixed in 4% paraformaldehyde in PBS for 10 min at room temperature, incubated for 10 min on ice with PBS containing 0.3% Triton X-100, and washed again 3 times with PBS. Thereafter, the coverslips were incubated for 20 min at 37 °C in PBS containing 5% goat serum, and washed again with PBS. Slides were stained using the PKH26 Red or PKH67 Green cell linker kits (Sigma) and incubated at room temperature for 10 min and then washed 4 times with PBS. After washes, slides were incubated for 5 min on ice in PBS containing DAPI (50 μg mL^{-1}), and then washed with PBS and mounted on glass slides. In the end, fluorescent signals were visualized with a fluorescence microscope (AXIO, Zeiss).

Results and discussion

Characterization of CNTs–PEI and CNTs–PEI/PVA

Raman spectroscopy was used to probe the structure of CNTs, CNTs–PEI and CNTs–PEI/PVA in the 110–2000 cm^{-1} region (Fig. 2), respectively.[61] The intensity ratio ($I_G : I_D$) of tangential mode (G band, 1500–1600 cm^{-1}) to the disorder mode (D band, 1300–1400 cm^{-1}) is often used to characterize functionalized CNTs.[61,62] The $I_G : I_D$ (2.6, 3.7 and 3.6, Fig. 2a) of CNTs, CNTs–PEI and CNTs–PEI/PVA. Compared to CNTs–COOH, the $I_G : I_D$ was increased after grafting with polymers. Under the

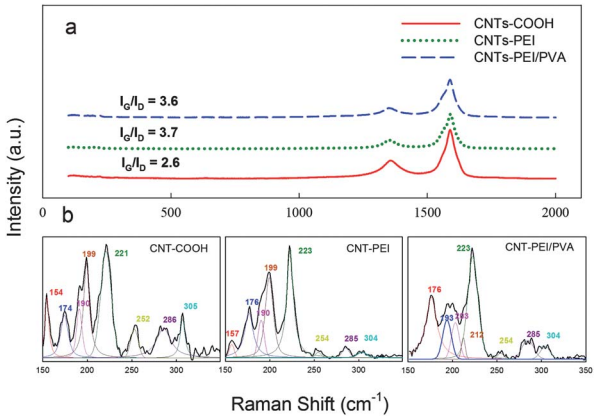

Fig. 2 Raman spectra of (a) CNTs–COOH, CNTs–PEI, and CNTs–PEI/PVA. (b) Radial Breathing Mode (RBM) and fitting peaks in the Raman spectra of CNTs–COOH, CNTs–PEI, and CNTs–PEI/PVA.

same conditions, the positions of the D bands remain unchanged, which may suggest the decrease of defects on the CNTs. The frequency and modal distribution of Radial Breathing Modes (RBM, 150–350 cm^{-1}) is the most important feature in characterizing the diameter and chirality of CNTs. After grafting with PEI and then complexing with PVA, there was a blue shift in the RBM and the intensities of peaks with smaller Raman shifts got weaker (Fig. 2b). This could be due to a case where the CNTs are no longer in contact with each other directly after successful grafting and complexation. Thermogravimetric analysis (TGA) (ESI, Fig. S2†) was used to characterize the surface modification of the CNTs.[6] For CNTs–COOH, there is no significant weight loss (12%) after the temperature is increased to 800 °C. However, at the same temperature, the weight loss of CNTs–PEI was 40%, and CNTs–PEI/PVA showed more than 45% weight loss.

The high-resolution transmission electronic microscopy (HR-TEM) was performed on a Titan 80–300 with accelerating voltage of 300 kV. HR-TEM was used to examine CNTs thickness after grafting and complexation. As expected, an increase of the polymer thickness was observed when comparing the CNTs–PEI (Fig. 3b) and CNTs–PEI/PVA (Fig. 3c) to CNTs–COOH (Fig. 3a). While the thickness of PEI on the CNT surface was around 0.9 nm, it was around 2 nm when PVA was complexed. The uniform amorphous polymer layer on the CNTs surface is clearly distinguished from the ordered walls of the CNTs–COOH. Moreover, electron energy loss spectroscopy (EELS, ESI, Fig. S3†) was also used to get more evidence of a successful grafting of PEI and complexation between PEI and PVA. From EELS results, the signals of N or O were observed after grafting or complexation. Scanning electron microscopy (SEM) observations were carried out on a Quanta 600 FEG scanning electron microscope (SEM, FEI Company). Compared to the initial CNTs–COOH (Fig. 3d), SEM images of the final product (Fig. 3e) show a good homogenous dispersion of CNTs and excellent control over the distance of CNTs by the zippered PEI/PVA complex.

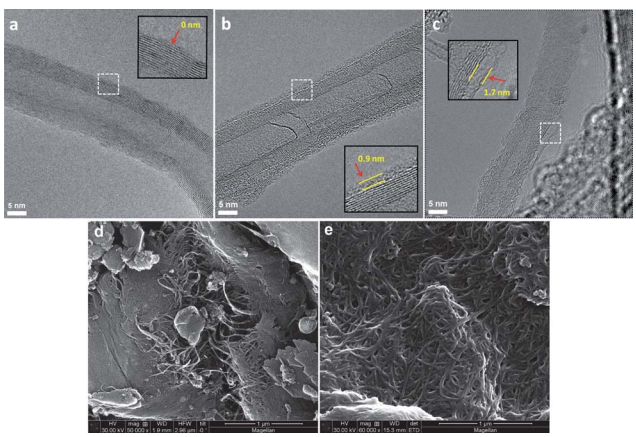

Fig. 3 High Resolution Transmission Electronic Microscopy (HR-TEM) of (a) CNTs–COOH, (b) CNTs–PEI, and (c) CNTs–PEI/PVA. The scale bar is 5 nm. Scanning Electron Microscopy (SEM) image of (d) CNTs–COOH and (e) CNTs–PEI/PVA. The scale bar is 1 μm.

Thermosensitive DOX release from CNTs–PEI/PVA

Operation of CNTs–PEI/PVA was first tested with Rhodamine B (RhB) before using DOX. The system successfully released RhB at elevated temperature while no release was observed at 25 °C (ESI, Fig. S4†). The system was then loaded with DOX and release curves (Fig. 4a) showed that DOX is stable in water at 25 °C; however, at body temperature (37 °C) there was a slow release. At high temperatures, *i.e.* 40 °C, the release of DOX was observed at a faster rate which increased at 70 °C. This behaviour is ascribed to the nature of hydrogen bonding between PEI and PVA, complexing at low temperature and decomplexing at high temperature.[41] As a control, DOX was loaded onto CNTs–COOH and CNTs–PEI similar to CNTs–PEI/PVA and then the systems were tested at 25 °C, 40 °C and 70 °C (Fig. 4b). The intensities are too weak to be estimated at ~585 nm (emission wavelength of DOX) and unchangeable, which show little DOX load efficiencies in these control samples after washing. The "on-off" switch experiments show the reversibility of DOX

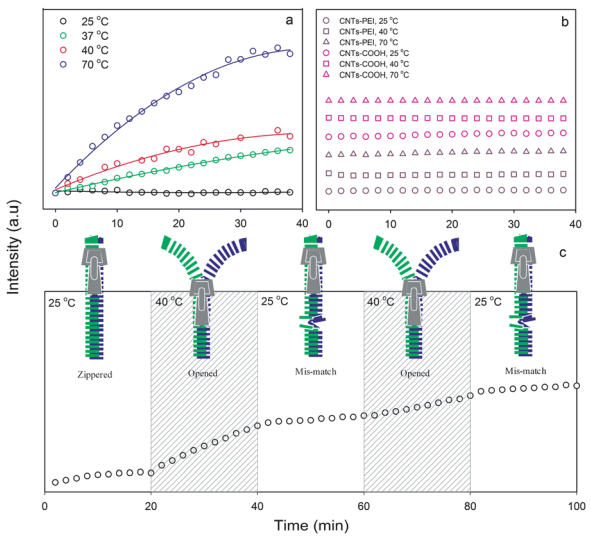

Fig. 4 (a) DOX release from CNTs–PEI/PVA at different temperatures. (b) No release from control samples (CNTs–COOH, CNTs–PEI at 25 °C, 40 °C and 70 °C). (c) Temperature sensitive "on-off" switch of CNTs–PEI/PVA.

temperature sensitive release. Going back to 25 °C, a little leakage of DOX exists, which is attributed to a mismatched "zipper" of PEI and PVA (Fig. 4c). The "on-off" experiment was first conducted at 40 °C (on) and 37 °C (off). Although a change in intensity could be seen, the slopes in the graph were too close to illustrate the difference. A plot of "on-off" switch at 40 °C (on) and 25 °C (off) shows clearly the system's temperature dependence (Fig. 4c).

Loading occurs by π–π interactions between CNTs and DOX that plays an important role in the initial loading. At a relative higher loading temperature (40 °C), the "zippers" are opened and DOX can penetrate the sparse polymeric network and attach to the surface of the CNTs. After the polymers are cooled down (25 °C), "zippers" are formed between PEI and PVA, which limit the free movement of the attached DOX. At this time, the high local concentration of DOX induces the quench of fluorescence. When the temperature is increased in the drug release experiment, the "zippers" are broken and the attached DOX could diffuse into the environment, causing the increasing of fluorescent signals. However, during the process of "on-off" switch experiments, "zippers" cannot be exactly recovered and are mismatched because of the nature of polymer chains, which induces the partial leakage of DOX. For the control samples, COOH groups or loose PEI polymers cannot hold DOX after washing. Poor loading efficiencies of DOX lead to unchangeable fluorescent intensities. Thus, polymer "zippers" are important to retain DOX on the CNTs and then control its release through thermosensitivity.

Thermosensitive *in vitro* DOX release and cell viability studies

To verify that CNTs–PEI/PVA are safe to use at different temperatures, we examined three different human cell lines (Lung fibroblast (LF), Breast Adenocarcinoma (BA) and HeLa) using two different methods, Alamar blue and LDH. Four sets of cells were placed in 96 well plates, and samples were treated in the following order: Control (no treatment), CNTs–PEI/PVA, DOX-loaded CNTs–PEI/PVA and DOX only (positive control). After a 48 h incubation at 37 °C, cell viability was assessed using the Alamar blue dye where the active metabolism of live cells can reduce the Alamar blue efficiently. As shown in Fig. 5b, results indicated that the CNTs treatment is not toxic to cells in both LF and BA; while in HeLa around 15% of cell death was observed compared to the untreated cells (control). Similar results were observed by the LDH method, where the cell death was very low (Fig. 5e).

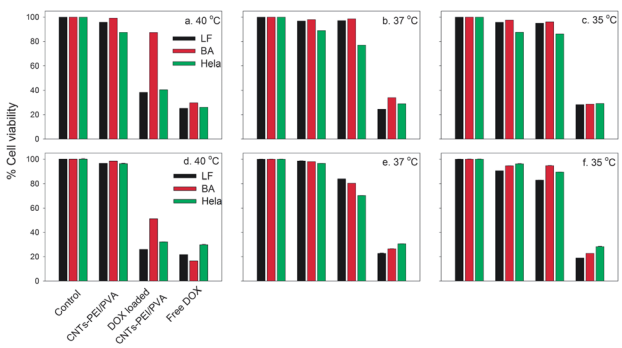

Fig. 5 Cell viability study at different temperatures. LF, BA and HeLa at (a) 40 °C (b) 37 °C (c) 35 °C using the Alamar blue method; LF, BA and HeLa at (d) 40 °C (e) 37 °C (f) 35 °C using the LDH method.

To further investigate the feasibility of CNTs–PEI/PVA as a drug delivery system, the same human cell lines (LF, and BA and HeLa) were used. Four sets of each cell line (6 wells each set) were placed in 96 well plates: untreated cells (negative control), cells treated with unloaded CNTs–PEI/PVA), cells treated with DOX loaded CNTs–PEI/PVA and DOX only (positive control). After 24 h the four cell sets of each cell line were incubated for three hours at 40 °C to aide the DOX release and a cell viability test was used to assess the effect on each treated cell line. As shown in Fig. 5, unloaded CNTs have no cytotoxic effect on cells. On the other hand, DOX loaded CNTs treatment caused more than 60% cell death in HeLa and LF (Fig. 5a, d). As for the BA, the percentage of cell death was about 30%. Furthermore, we tested the effect of the CNTs on healthy primary cells, (Human Dermal Fibroblast adult (HDFa) and Human Dermal Fibroblast neonatal (HDFn)), unloaded CNTs have no cytotoxic effect on primary cells while DOX loaded CNTs treatment caused more than 70% cell death (ESI, Fig. S5†).

Based on previous observations, we compared the CNTs drug delivery efficiency at 35 °C (Fig. 5c, f) and 37 °C (Fig. 5b, e) to the efficiency at 40 °C (Fig. 5a, d). Results show that the polymer-gated CNTs did not deliver the drug efficiently at 35 °C and 37 °C in comparison to the results at 40 °C. Although, BA and LF treated cell survival rates were almost equal to untreated cells at 35 °C and 37 °C, HeLa treated cells showed an average of 30% survival rates less than the untreated ones at the same temperatures. These results indicate that CNTs work more efficiently at temperatures higher than 37 °C, which can help the CNTs specificity in delivering the drug to tumors since they display higher temperatures than the normal body tissues (37 °C).[63] Moreover, the system can be triggered using an external heating source.

Cellular uptake of DOX

CNTs-PEI/PVA which were loaded with DOX were further incubated with Breast Adenocarcinoma (BA) cells for 2.5 h at 35 °C, 37 °C and 40 °C, and analyzed by fluorescence microscopy. CNTs–PEI/PVA were well dispersed in cell culture media, however, aggregates (ESI, Fig. S6†) were also seen and this is due to the nature of the CNTs.[64] Gentle sonication for 5–10 min helped in decreasing CNT aggregation. DOX can be easily located in cells due to its red fluorescence as it can be seen in Fig. 6a4, b4 and c4 where merged images of the bright field and DOX are represented. The nuclei were stained with DAPI (blue, Fig. 6a3, b3 and c3), and merged views of the bright field and DOX with the nuclei are represented in Fig. 6a5, b5 and c5.

Comparing the uptake of DOX at the three different temperatures, it can be seen clearly that the intensity of the DOX at 35 °C (Fig. 6a) is lower than the intensity at 37 °C (Fig. 6b). As it is expected that at 37 °C the system will be opened more than at 35 °C, and consequently it will release more DOX. At 40 °C (Fig. 6c), we did not see an increase in fluorescence intensity as many dead cells were washed away during sample preparation. This result is coherent with the drug uptake study presented in Fig. 5.

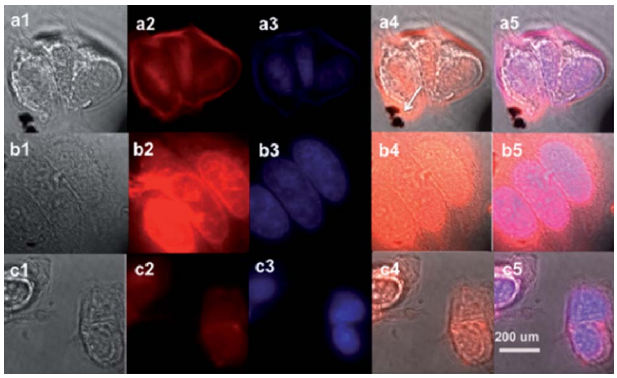

Fig. 6 Fluorescence microscopy images of BA cells incubated with CNTs–PEI/PVA at (a) 35 °C, (b) 37 °C, and (c) 40 °C. They show the uptake of DOX (red) and the nuclei (blue), which were stained with DAPI. A1, b1 and c1 are the bright field images of BA cells. A2, b2 and c2 are images of red DOX. A3, b3 and c3 are images of blue nuclei. A4, b4 and c4 are merged images of the bright field and DOX. A5, b5 and c5 are merged images of the bright field, DOX and DAPI. 200 μm is the scale bar for all the images.

Conclusions

A temperature sensitive drug delivery system based on polymer-gated CNTs is reported. The hydrogen bonding between PEI and PVA controlled the release of loaded DOX (34.128 μg mg^{-1}). The release of DOX was tested in different cell lines (LF, BA, HeLa, HDFa and HDFn) under different temperatures. The hydrogen bonds were decomplexed at 40 °C, which allowed the drug to be released. On the other hand, no release was observed at 25 °C and slow release at 37 °C. Preliminary results showed that this system is safe and can be potentially useful in future CNT drug delivery applications.

Acknowledgements

The research presented is fully sponsored by King Abdullah University of Science and Technology (KAUST). We thank Dr. Mustafa Ali for all the support and helpful discussions.

References

1 R. H. Baughman, A. A. Zakhidov and W. A. de Heer, *Science*, 2002, **297**, 787–792.
2 M. F. Yu, B. S. Files, S. Arepalli and R. S. Ruoff, *Phys. Rev. Lett.*, 2000, **84**, 5552–5555.
3 J. N. Coleman, U. Khan, W. J. Blau and Y. K. Gun'ko, *Carbon*, 2006, **44**, 1624–1652.
4 S. Iijima, *Nature*, 1991, **354**, 56–58.
5 Y. T. Park, A. Y. Ham and J. C. Grunlan, *J. Phys. Chem. C*, 2010, **114**, 6325–6333.
6 M. N. Ahmad, M. Nadeem, Y. H. Ma and W. T. Yang, *J. Mater. Sci.*, 2010, **45**, 5591–5597.
7 M. S. Dresselhaus, G. Dresselhaus, J. C. Charlier and E. Hernandez, *Philos. Trans. R. Soc. London, Ser. A*, 2004, **362**, 2065–2098.
8 F. Rivadulla, C. Mateo-Mateo and M. A. Correa-Duarte, *J. Am. Chem. Soc.*, 2010, **132**, 3751–3755.
9 F. Caruso, *Adv. Mater.*, 2001, **13**, 11–22.
10 A. Thess, R. Lee, P. Nikolaev, H. J. Dai, P. Petit, J. Robert, C. H. Xu, Y. H. Lee, S. G. Kim, A. G. Rinzler, D. T. Colbert, G. E. Scuseria, D. Tomanek, J. E. Fischer and R. E. Smalley, *Science*, 1996, **273**, 483–487.
11 F. Liang and B. Chen, *Curr. Med. Chem.*, 2010, **17**, 10–24.
12 J. T. Hu, T. W. Odom and C. M. Lieber, *Acc. Chem. Res.*, 1999, **32**, 435–445.
13 J. C. Grunlan, Y. T. Park and A. Y. Ham, *J. Phys. Chem. C*, 2010, **114**, 6325–6333.
14 Z. X. Jin, Q. C. Zhao, X. D. Feng and S. L. Mei, *Nanotechnology*, 2009, **20**, 1–8.
15 E. P. Dillon, C. A. Crouse and A. R. Barron, *ACS Nano*, 2008, **2**, 156–164.
16 T. Panczyk, T. P. Warzocha and P. J. Camp, *J. Phys. Chem. C*, 2010, **114**, 21299–21308.
17 A. Bianco, K. Kostarelos and M. Prato, *Curr. Opin. Chem. Biol.*, 2005, **9**, 674–679.
18 J. Yun, J. S. Im, Y. S. Lee, T. S. Bae, Y. M. Lim and H. I. Kim, *Colloids Surf., A*, 2010, **368**, 23–30.
19 V. V. Chaban, T. I. Savchenko, S. M. Kovalenko and O. V. Prezhdo, *J. Phys. Chem. B*, 2010, **114**, 13481–13486.
20 Q. C. Zhao, X. D. Feng, S. L. Mei and Z. X. Jin, *Nanotechnology*, 2009, **20**, 1–8.
21 R. P. Feazell, N. Nakayama-Ratchford, H. Dai and S. J. Lippard, *J. Am. Chem. Soc.*, 2007, **129**, 8438–8439.
22 J. Y. Chen, S. Y. Chen, X. R. Zhao, L. V. Kuznetsova, S. S. Wong and I. Ojima, *J. Am. Chem. Soc.*, 2008, **130**, 16778–16785.
23 A. Nunes, N. Amsharov, C. Guo, J. Van den Bossche, P. Santhosh, T. K. Karachalios, S. F. Nitodas, M. Burghard, K. Kostarelos and K. T. Al-Jamal, *Small*, 2010, **6**, 2281–2291.
24 Z. Liu, X. M. Sun, N. Nakayama-Ratchford and H. J. Dai, *ACS Nano*, 2007, **1**, 50–56.
25 M. Prato, D. Pantarotto, R. Singh, D. McCarthy, M. Erhardt, J. P. Briand, K. Kostarelos and A. Bianco, *Angew. Chem., Int. Ed.*, 2004, **43**, 5242–5246.
26 B. D. Chen, H. Zhang, C. X. Zhai, N. Du, C. Sun, J. W. Xue, D. R. Yang, H. Huang, B. Zhang, Q. P. Xie and Y. L. Wu, *J. Mater. Chem.*, 2010, **20**, 9895–9902.
27 L. L. del Mercato, P. Rivera-Gil, A. Z. Abbasi, M. Ochs, C. Ganas, I. Zins, C. Sonnichsen and W. J. Parak, *Nanoscale*, 2010, **2**, 458–467.
28 P. Pantano, S. F. Chin, R. H. Baughman, A. B. Dalton, G. R. Dieckmann, R. K. Draper, C. Mikoryak, I. H. Musselman, V. Z. Poenitzsch and H. Xie, *Exp. Biol. Med.*, 2007, **232**, 1236–1244.
29 P. A. Wender, N. W. S. Kam, T. C. Jessop and H. J. Dai, *J. Am. Chem. Soc.*, 2004, **126**, 6850–6851.
30 K. Kostarelos, L. Lacerda, G. Pastorin, W. Wu, S. Wieckowski, J. Luangsivilay, S. Godefroy, D. Pantarotto, J. P. Briand, S. Muller, M. Prato and A. Bianco, *Nat. Nanotechnol.*, 2007, **2**, 108–113.
31 H. J. Dai, Z. Liu, C. Davis, W. B. Cai, L. He and X. Y. Chen, *Proc. Natl. Acad. Sci. U. S. A.*, 2008, **105**, 1410–1415.
32 A. A. Bhirde, V. Patel, J. Gavard, G. F. Zhang, A. A. Sousa, A. Masedunskas, R. D. Leapman, R. Weigert, J. S. Gutkind and J. F. Rusling, *ACS Nano*, 2009, **3**, 307–316.
33 H. J. Dai, S. Dhar, Z. Liu, J. Thomale and S. J. Lippard, *J. Am. Chem. Soc.*, 2008, **130**, 11467–11476.
34 J. L. Kong, X. X. Weng, M. Y. Wang, J. Ge, S. N. Yu, B. H. Liu and J. Zhong, *Mol. BioSyst.*, 2009, **5**, 1224–1231.
35 D. E. Bergbreiter and B. S. Chance, *Macromolecules*, 2007, **40**, 5337–5343.
36 G. Greene, G. Yao and R. Tannenbaum, *Langmuir*, 2004, **20**, 2739–2745.
37 S. Y. Yang and M. F. Rubner, *J. Am. Chem. Soc.*, 2002, **124**, 2100–2101.
38 G. Z. Wu, D. W. Long and G. L. Zhu, *Int. J. Mol. Sci.*, 2008, **9**, 120–130.
39 H. Shirota and K. Horie, *Macromol. Symp.*, 2004, **207**, 79–93.
40 G. K. Such, A. P. R. Johnston and F. Caruso, *Chem. Soc. Rev.*, 2011, **40**, 19–29.
41 Z. C. Li, L. Deng, C. H. Wang and D. H. Liang, *Macromolecules*, 2010, **43**, 3004–3010.
42 Q. H. Lu, X. K. Zhang, L. J. Meng, Z. F. Fei and P. J. Dyson, *Biomaterials*, 2009, **30**, 6041–6047.
43 M. Fujiwara, N. K. Mal and Y. Tanaka, *Nature*, 2003, **421**, 350–353.
44 M. Fujiwara, N. K. Mal, Y. Tanaka, T. Taguchi and M. Matsukata, *Chem. Mater.*, 2003, **15**, 3385–3394.
45 R. Martinez-Manez, R. Casasus, E. Climent, M. D. Marcos, F. Sancenon, J. Soto, P. Amoros, J. Cano and E. Ruiz, *J. Am. Chem. Soc.*, 2008, **130**, 1903–1917.

46 D. S. Kohane, T. Hoare, B. P. Timko, J. Santamaria, G. F. Goya, S. Irusta, S. Lau, C. F. Stefanescu, D. B. Lin and R. Langer, *Nano Lett.*, 2011, **11**, 1395–1400.
47 J. F. Stoddart, S. Angelos, Y. W. Yang, K. Patel and J. I. Zink, *Angew. Chem., Int. Ed.*, 2008, **47**, 2222–2226.
48 J. I. Zink, N. M. Khashab, M. E. Belowich, A. Trabolsi, D. C. Friedman, C. Valente, Y. N. Lau, H. A. Khatib and J. F. Stoddart, *Chem. Commun.*, 2009, 5371–5373.
49 X. Yang, B. A. Moosa, L. Deng, L. Zhao and N. M. Khashab, *Polym. Chem.*, 2011, **2**, 2543–2547.
50 J. F. Stoddart, S. Angelos, N. M. Khashab, Y. W. Yang, A. Trabolsi, H. A. Khatib and J. I. Zink, *J. Am. Chem. Soc.*, 2009, **131**, 12912–12914.
51 J. I. Zink, K. Patel, S. Angelos, W. R. Dichtel, A. Coskun, Y. W. Yang and J. F. Stoddart, *J. Am. Chem. Soc.*, 2008, **130**, 2382–2383.
52 A. Heise and P. D. Thornton, *J. Am. Chem. Soc.*, 2010, **132**, 2024–2028.
53 C. Kim, C. Park, H. Kim and S. Kim, *J. Am. Chem. Soc.*, 2009, **131**, 16614–16615.
54 W. Huang, J. Y. Liu, Y. Pang, Z. Y. Zhu, X. Y. Zhu, Y. F. Zhou and D. Y. Yan, *Biomacromolecules*, 2011, **12**, 2407–2415.
55 K. H. Yoo, H. Park, J. Yang, J. Lee, S. Haam and I. H. Choi, *ACS Nano*, 2009, **3**, 2919–2926.
56 N. J. Halas, R. Huschka, O. Neumann and A. Barhoumi, *Nano Lett.*, 2010, **10**, 4117–4122.
57 J. F. Stoddart, S. Angelos, Y. W. Yang, N. M. Khashab and J. I. Zink, *J. Am. Chem. Soc.*, 2009, **131**, 11344–11346.
58 J. F. Stoddart, T. D. Nguyen, Y. Liu, S. Saha, K. C. F. Leung and J. I. Zink, *J. Am. Chem. Soc.*, 2007, **129**, 626–634.
59 H. Hu, Y. C. Ni, S. K. Mandal, V. Montana, N. Zhao, R. C. Haddon and V. Parpura, *J. Phys. Chem. B*, 2005, **109**, 4285–4289.
60 M. W. Shen, S. H. Wang, X. Y. Shi, X. S. Chen, Q. G. Huang, E. J. Petersen, R. A. Pinto, J. R. Baker and W. J. Weber, *J. Phys. Chem. C*, 2009, **113**, 3150–3156.
61 R. Saito, T. Takeya, T. Kimura, G. Dresselhaus and M. S. Dresselhaus, *Phys. Rev. B: Condens. Matter*, 1998, **57**, 4145–4153.
62 R. Graupner, *J. Raman Spectrosc.*, 2007, **38**, 673–683.
63 Q. Zhao, J. M. Zhang, R. Wang and W. Cong, *IEEE Eng. Med. Biol. Mag.*, 2008, **27**, 64–66.
64 M. Ozkan and N. G. Portney, *Anal. Bioanal. Chem.*, 2006, **384**, 620–630.

